Distortion definition and correction in off-axis systems

Da Deppo, Vania, Simioni, Emanuele, Naletto, Giampiero, Cremonese, Gabriele

Vania Da Deppo, Emanuele Simioni, Giampiero Naletto, Gabriele Cremonese, "Distortion definition and correction in off-axis systems," Proc. SPIE 9626, Optical Systems Design 2015: Optical Design and Engineering VI, 962634 (23 September 2015); doi: 10.1117/12.2191332

SPIE.

Event: SPIE Optical Systems Design, 2015, Jena, Germany

Distortion definition and correction in off-axis systems

Vania Da Deppo*[a,b], Emanuele Simioni[a], Giampiero Naletto[c,a,b,d], Gabriele Cremonese[b]

[a] CNR-Institute for Photonics and Nanotechnologies UOS Padova LUXOR, Via Trasea 7, 35131 Padova, Italy
[b] INAF-Osservatorio Astronomico di Padova, Vicolo dell'Osservatorio 5, 35122 Padova, Italy
[c] Dept. of Information Engineering, University of Padova, Via Gradenigo 6/B, 35131 Padova, Italy
[d] CISAS G. Colombo, University of Padova, Via Venezia 15, 35131 Padova, Italy

ABSTRACT

Off-axis optical configurations are becoming more and more used in a variety of applications, in particular they are the most preferred solution for cameras devoted to Solar System planets and small bodies (i.e. asteroids and comets) study. Off-axis designs, being devoid of central obstruction, are able to guarantee better PSF and MTF performance, and thus higher contrast imaging capabilities with respect to classical on-axis designs. In particular they are suitable for observing extended targets with intrinsic low contrast features, or scenes where a high dynamical signal range is present.

Classical distortion theory is able to well describe the performance of the on-axis systems, but it has to be adapted for the off-axis case.

A proper way to deal with off-axis distortion definition is thus needed together with dedicated techniques to accurately measure and hence remove the distortion effects present in the acquired images.

In this paper, a review of the distortion definition for off-axis systems will be given. In particular the method adopted by the authors to deal with the distortion related issues (definition, measure, removal) in some off-axis instruments will be described in detail.

Keywords: distortion, off-axis systems, calibration, optical simulation

1. INTRODUCTION

Conventional reflecting telescopes, such as Newtonian and Cassegrain, and all the various catadioptrics, such as Schmidt and Maksutov, have a central obstruction in their light path due to secondary mirror or focal plane assembly (FPA). In some designs further obstruction is induced by the support structures, such as spiders, necessary to hold the secondary mirror or FPA in place. The effect on the image due to the obstruction of the incoming light beam is evident in the PSF and MTF of a system. Increasing the obstruction ratio, the light diffracted in the primary Airy disk decreases, while it increases in the diffraction rings [1], and the MTF response with respect to object spatial frequency decreases rapidly with increasing obstruction ratio [2]. Thus obscured systems exhibit a resulting contrast loss. This effect is particularly detrimental in imaging extended objects having a low inherent contrast, such as Solar System planets and small bodies (i.e. asteroids and comets) surfaces, or when very faint details are to be detected near to a bright source, such as cometary dust and gas coma features near a bright nucleus limb.

For all the applications in which a high contrast imaging capability is necessary, an unobscured design has to be taken into account. To avoid obscuration, off-axis design solutions have to be considered. Unobscured off-axis telescope designs may be classified basically into three types.

The eccentric pupil class, where an ordinary coaxial design is used with an eccentric stop (see sketch in Figure 1a). All the optical elements have a common optical axis and the center of view direction is parallel to the optical axis. The principal (chief) ray of the beam at the center of the FoV is not coincident with the common optical axis but it is shifted. Common design examples for this class are the off-axis paraboloid and off-axis Schmidt telescope.

The off-axis FoV class, where an off-axis FoV portion of an ordinary coaxial design (see sketch in Figure 1b) is used. The center of view direction is tilted with respect to the common optical axis.

*vania.dadeppo@ifn.cnr.it; phone +39-049 9815639; fax +39-049 774627

Optical Systems Design 2015: Optical Design and Engineering VI, edited by Laurent Mazuray, Rolf Wartmann, Andrew P. Wood, Proc. of SPIE Vol. 9626, 962634 · © 2015 SPIE · CCC code: 0277-786X/15/$18 · doi: 10.1117/12.2191332

The tilted and decentered component telescope (TCT) (see sketch in Figure 1c), in which each optical element is rotationally symmetric about its own optical axis which may be tilted and/or decentered with respect to the optical axis of the other optical elements. Common TCT designs used in amateur astronomy are Schiefspiegler and Yolo [3].

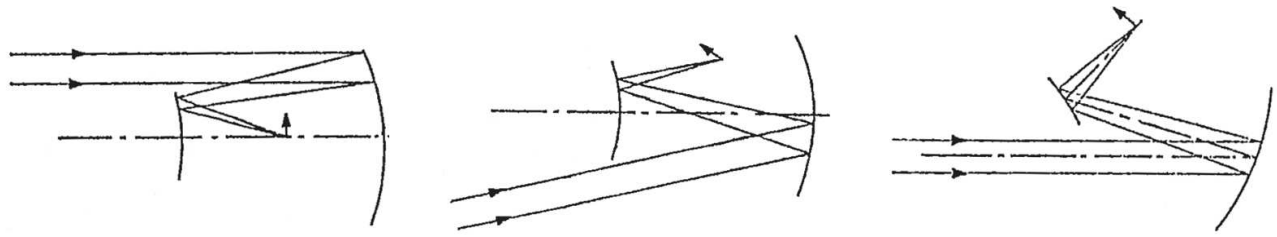

(a) (b) (c)

Figure 1. Common classification for off-axis designs. (a) Eccentric pupil. (b) Off-axis FoV. (c) Tilted-component telescope.

2. DISTORTION DEFINITION

2.1 Distortion concept

Distortion is usually referred to as the last of the five monochromatic aberrations [4] and it is a concept more complex than usually assumed. Distortion is defined as the displacement, on the focal plane, between the real position of the image of an object point and the theoretical Gaussian one. It does not affect the quality of the image in itself, i.e. a point source is still imaged in a point sharply in focus, but the image position differs from paraxial theory prediction.

This image aberration is associated to a variation of the optical system magnification with the field position. In fact, considering for the sake of drawing simplicity a planar situation as in Figure 2a, given an object point height y, the paraxial magnification is $M_p = y_p'/y$, where y_p' is the paraxial image height. If the real image height is $y' \neq y_p'$ the real magnification is $M = y'/y \neq M_p$.

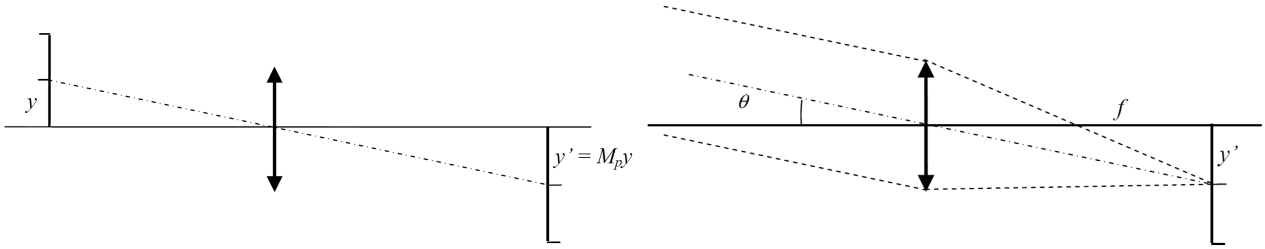

(a) (b)

Figure 2. (a) Sketch showing the relation between object and image height for a system working at finite conjugate. (b) Sketch showing the relation between FoV angle and image height for an instrument working with the object at infinity.

If the magnification does not vary with the field, $M = M_p$, i.e. no distortion is present: the image of the object is simply an M_p-scaled replica of the object (the image maintains exactly the same proportions of the object).

If the object plane is at infinity (see Figure 2b), a different description has to be adopted. The height of the object cannot be determined and the position of the point in the FoV is defined by the angle (θ) that the beam forms with the system optical axis. The paraxial image height is given by the relation:

$$y_p' = f \tan\theta \quad (1)$$

where f is the focal length of the system. With respect to the previous definition used for a system imaging a near object, the object size has to be substituted with angular subtense and the magnification with the focal length [5].
In an actual optical system working at finite conjugate the transverse magnification may be function of the off-axis object distance (y), or, for a system working with object at infinity, the focal length may vary with the angle θ that the principal ray forms with the optical axis. For this reason, different positions in the system FoV can feature different focal lengths and different magnifications.

2.2 Distortion description in on-axis axial symmetric systems

When imaged by an ideal optical system, a square grid is exactly a scaled version of the object (as in Figure 3a), and the image has no distortion aberration. Actually, with common axial symmetric optical systems, the grid can be distorted in a pincushion way, also called positive distortion, (see Figure 3b), or in a barrel one, called negative distortion, (see Figure 3c).

Here we are taking into account a system free of all the aberrations except distortion and thus each object point is considered to be perfectly imaged in an image point and the center, chosen as the reference point of the pattern, corresponds to the image of the object point placed on the system optical axis.

For positive distortion the image points are displaced radially outward from the center, for negative distortion they are displaced radially toward the center, with the most distant point from the center moving the greatest amount. Pincushion distortion corresponds to the case in which the magnification of the system increases from the center to the edges of the FoV, while barrel distortion has a decreasing magnification from the center outward.

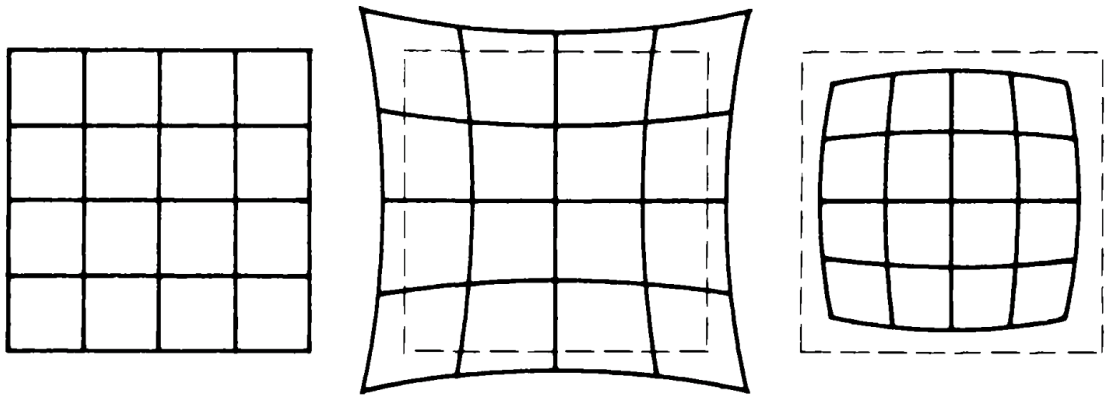

(a) (b) (c)

Figure 3. Classical distortion description. (a) Undistorted image of a grid pattern object. (b) Pincushion (positive) distortion. (c) Barrel (negative) distortion.

The amount of distortion for a point in the FoV in a circular symmetric system is described by the percentage of the displacement between the real and the paraxial image radial position. If h_r is the real chief ray distance on the image plane measured with respect to the optical axis, and h_p is the paraxial one, the distortion on the image plane position h_r is:

$$\frac{h_r - h_p}{h_p} \times 100 \quad (2)$$

This simple description is well suited for rotational symmetric systems but not for asymmetric ones. Moreover the distortion in real systems is much more complicated with respect to this simple model.

2.3 Description of the distortion in off-axis systems

The distortion behaviour in off-axis systems can be easily grasped if an off-axis FoV portion of an on-axis rotational symmetric system is taken into account. As depicted in Figure 4, to a first approximation, a square object element placed off-axis in the object plane is imaged as a trapezoidal element in the off-axis distorted image.

For an off-axis system with original on-axis pincushion distortion, the magnification and the focal length are increasing with the distance from the axis, which results in an increase of the focal length both in x and y direction. The internal side of the square, i.e. the one nearer to the optical axis, is less magnified than the external one (see Figure 4b). The opposite is happening for barrel distortion (see Figure 4c), the magnification and the focal length are decreasing outward thus the internal side of the square is longer than the external one. This effect is usually called keystone distortion [6].

Looking at the effect more deeply, smile, or bowing, distortion is present since the lines are mapped into curved segments, both in x and y directions (see Figure 5).

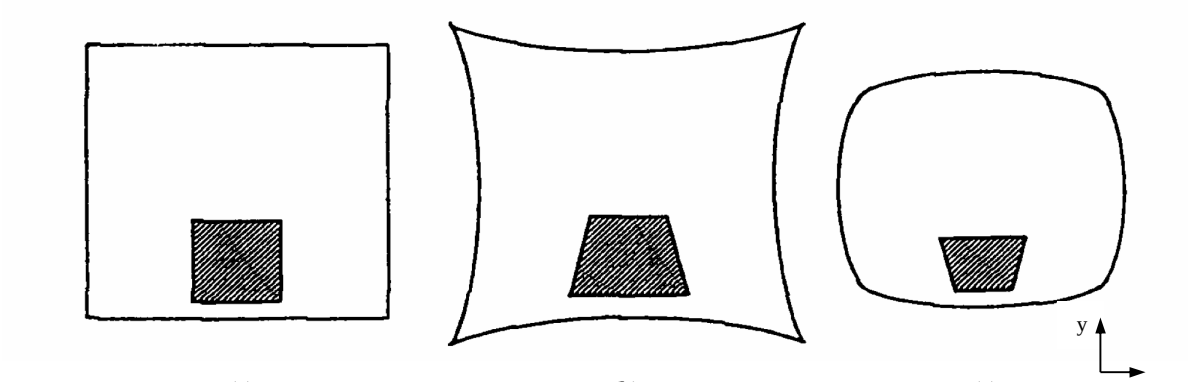

(a) (b) (c)

Figure 4. Distortion sketches for off-axis systems. (a) Undistorted image of a square object placed off-axis. (b) Pincushion or positive distortion. (c) Barrel or negative distortion.

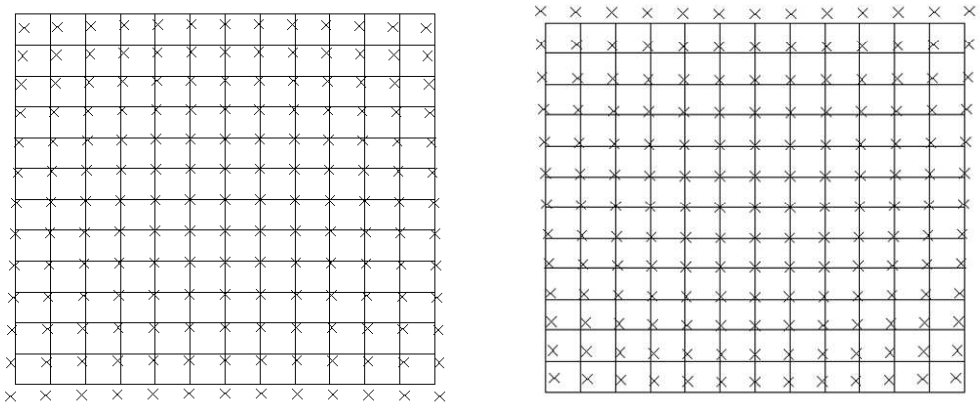

(a) (b)

Figure 5. Distortion for off-axis systems. The distorted point positions (×) are plotted against the expected undistorted grid. (a) Pincushion distortion (b) Barrel distortion.

3. DISTORTION MODEL IN OFF-AXIS SYSTEMS

3.1 Reference models or ideal camera models

As stated in the previous section, the distortion is defined as the measurement of the shift of the real image of a point with respect to the nominal reference case, which is assumed to be the paraxial one. For wide angle and off-axis systems it is not always clear what the reference to which the distortion has to be calculated and measured is; and, depending on the applications, in which way the image has to be undistorted to get the optimal imaging [7].

The imaging geometry of most cameras can be described as a two-stage process: projection of the 3D world onto a unit sphere (the *viewing sphere*) followed by a projection of the sphere onto the image plane. There are many reasonable choices for projection onto the image plane [8], here we mention two of them which are relevant for astronomical applications. The *perspective* projection:

$$y' = k \tan\vartheta \tag{3}$$

which corresponds to the nominal paraxial case, in which the projection is function of the incoming angle ϑ, and the *equidistant* projection:

$$y' = k\,\vartheta, \tag{4}$$

where k is a scaling constant, equal to the focal length for object at infinity. For narrow angle imaging, the two models are very similar, but they can be extremely different far from the optical axis.

Obviously an image corrected for perspective or for equidistant projection will appear different. The reference model for a camera has to be chosen having in mind the application for which the instrument has been developed.

The perspective projection, also called F-Tan(Theta), preserves the straightness of the lines. It is normally used for extended scenes, but if the FoV is rather large, the same object viewed either at the center or at the edges of the FoV will have different sizes and will be perceived as deformed. Equidistant projection, also called F-Theta, is useful in applications where angular positions are to be measured, such as astrometry, or in laser scanning systems [9]. As for the applications presented in this paper only the perspective projection will be considered.

3.2 From on-axis to off-axis description

The first method which can be thought of to deal with distortion in an off-axis system is simply to describe it as the distortion of the off-axis portion of an original on-axis system; thus the input angles are referred to the original optical axis of the instrument and the on-axis focal length is the reference. In this way the object plane is considered to be orthogonal to the original optical axis of the system and the reference focal length is chosen in a point which is outside the real FoV.

An alternative approach is to define a new tilted reference axis, which can coincide with the boresight of the instrument, or with the chief ray of the center of the FoV, or with the chief ray of the beam impinging on the center of the detector or on a specified selected pixel, etc. In this way the object plane is selected to be orthogonal to the new reference axis, and also the incidence angles are measured with respect to this reference axis. Usually this new reference axis is also assumed to be the z axis of the reference system.

When doing this, i.e. changing the reference system from on-axis to off-axis choosing some field point as the reference axis, distortion must be re-evaluated. It is proper to define tangential and sagittal distortions, the two being mutually perpendicular. Points above and below the center (as well as left to right in a system which is off-axis in both x and y direction) are not symmetrical about the center of the FoV. To a first approximation, a circular object centered on the new reference axis will be re-imaged as an ellipse with its axes proportional to the tangential and sagittal focal lengths at the center of the image.

To better describe the system in this case, it is preferable to disentangle the tangential and sagittal planes, introducing a reference system with x and y directions related to sagittal and tangential planes. This allows to take into account the anamorphic effects in which the tangential and sagittal focal lengths, or magnifications, are different.

The position on the image plane can be defined, for systems working at finite conjugate, as:

$$\begin{aligned} x_i &= M_s\, x_o \\ y_i &= M_t\, y_o \end{aligned} \tag{5}$$

where x_i and y_i are the image coordinates on the image plane, x_o and y_o are those of the object in the object plane and M_s and M_t are respectively the magnification in the sagittal (xz) and tangential (yz) planes.

For systems working with object at infinity it can be written:

$$\begin{aligned} x_i &= f_s \tan\vartheta_x \\ y_i &= f_t \tan\vartheta_y \end{aligned} \tag{6}$$

with f_s and f_t the focal lengths respectively in the sagittal and the tangential planes, and ϑ_x and ϑ_y the angles of the incoming chief rays in the sagittal and the tangential planes. More generally we can write:

$$\begin{aligned} x_i &= k_s\ \tan\vartheta_x \\ y_i &= k_t\ \tan\vartheta_y \end{aligned} \tag{7}$$

where the object point, no matter how it is at finite or infinity, is described by the angles of the incoming chief rays and the k are scaling constants.

In order to describe more complicated systems, the following model can be taken into account:

$$\begin{pmatrix} x_i \\ y_i \end{pmatrix} = \begin{bmatrix} A & B \\ C & D \end{bmatrix} \begin{pmatrix} \tan\vartheta_x \\ \tan\vartheta_y \end{pmatrix} \tag{8}$$

where the elements of the matrix, ABCD, can be expressed as polynomial expressions as a function of either the image coordinates or the incoming angles.

Obviously, the model can be inverted to determine the input angles or coordinates from the image position coordinates:

$$\begin{pmatrix} \tan\vartheta_x \\ \tan\vartheta_y \end{pmatrix} = \begin{bmatrix} A & B \\ C & D \end{bmatrix}^{-1} \begin{pmatrix} x_i \\ y_i \end{pmatrix} \tag{9}$$

4. DISTORTION CALCULATION EXAMPLES

4.1 Introduction

In this work we describe the method adopted for the distortion analysis for two specific off-axis configurations. The first case considered is a wide angle camera designed for the imaging system OSIRIS [10] on board the ESA Rosetta mission; the second one a stereo camera (STC-SIMBIOSYS [11]) conceived for the 3D reconstruction of the planet Mercury surface in the framework of the ESA-JAXA BepiColombo mission.

4.2 Distortion analysis for the WAC on board the Rosetta ESA mission

The Wide Angle Camera (WAC) on board the Rosetta mission is one of the two cameras of the OSIRIS imaging instrument, which aims to study the evolution of a comet surface and its activity during part of its orbit around the Sun.

The WAC has been specifically designed to image the nucleus of the comet and the dust and gas environment around it [12]. To be able to see the weak coma features near the bright nucleus, a high contrast ratio is needed; the chosen optical design is an all-reflective, two-mirror, 20° off-axis, unobstructed and unvignetted one (see Figure 6).

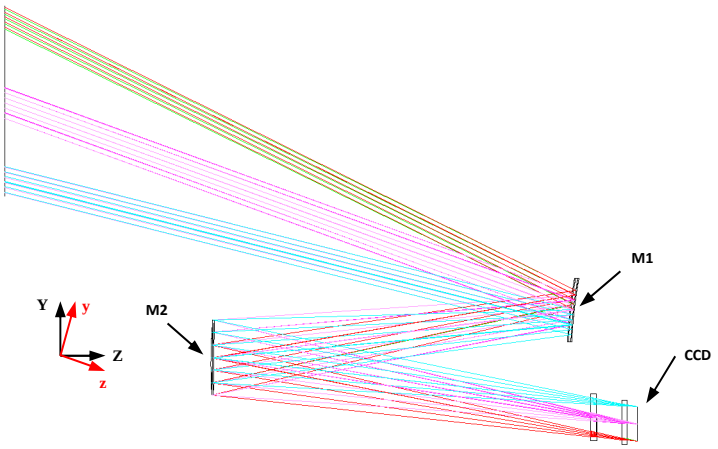

Figure 6. WAC optical layout. The axes directions (XYZ) of the original optical axis reference system and the ones (xyz) of the boresight reference system are indicated.

This camera is a typical example of an off-axis FoV design: both the primary (M1) and the secondary mirror (M2) share the same optical axis, but the useful FoV is centered around a direction tilted by 20° with respect to this axis. For M1 only an off-axis portion is used, while the secondary mirror (M2), which is the system aperture stop, is centered. The design is a kind of a Schmidt camera with a reflective corrector (M1).

The simplest camera model that can be taken into account is the so called “simplified pinhole model”, which corresponds to an ABCD model with $A=D=f$ and $B=C=0$, (the skew coefficient is null for the considered application). If the distortion is calculated with respect to the original optical axis and focal length, i.e. 140 mm, a -10.5% maximum distortion is found (see Figure 7a). But, as already mentioned, this method has no practical significance since the reference on-axis point is not inside the useful FoV of the system.

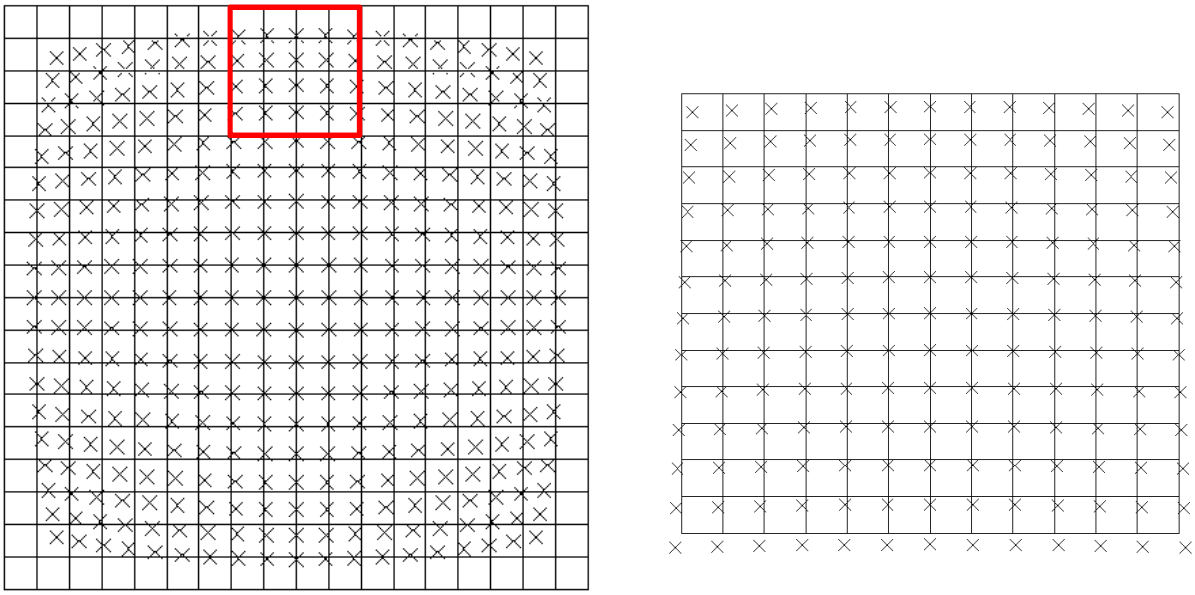

(a) (b)

Figure 7. (a) WAC distortion defined in the reference system of the original optical axis (the bold upper square indicates the portion of the useful FoV). (b) WAC distortion defined in the reference system centered on the 20° off-axis FoV; the whole useful FoV has been depicted and anamorphic distortion has been subtracted. The real positions (×) are superimposed on the reference non distorted grids.

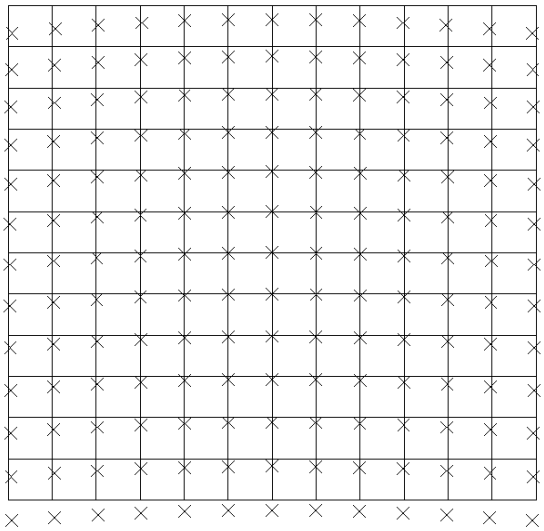

Figure 8. WAC distortion defined in the reference system of the boresight direction. The grid corresponds to the ideal non-distorted image; the crosses (×) represent the distorted images of the vertexes of the grid. Note that the differences between the real and ideal positions have been multiplied by a factor of 5 to make the distortion effect more evident.

As a first step, we can move the reference point in the FoV to the 20° off-axis boresight direction. This is simply done considering the following equation:

$$\begin{pmatrix} x_{\mathrm{i}} \\ y_{\mathrm{i}} - y_{20} \end{pmatrix} = \begin{bmatrix} A & B \\ C & D \end{bmatrix} \begin{pmatrix} \tan\vartheta_x \\ \tan\vartheta_y - \tan 20° \end{pmatrix} \tag{10}$$

where y_{20} corresponds to the y image position coordinate of the $(\vartheta_x,\vartheta_y)$ = (0°,20°) incoming beam. The reference object plane is still orthogonal to the original reference optical axis. To account for anamorphic distortion, the sagittal and

tangential focal lengths are respectively $A = 116$ mm and $D = 131.5$ mm. A maximum distortion of -6% is present (see Figure 7b).

A further step, after having changed the position of the center of the reference system, is to rotate the reference system to consider the line of sight as the reference axis. Therefore the reference object plane will be orthogonal to the line of sight, that is the preferred solution in most applications. In the rotated reference system, the angular directions of the reference grid are different from the previous cases and the pattern of the distortion is actually changed (see Figure 8). In this picture the effects of the distortion have been multiplied by a factor of 5 in order to be clearly visible. The maximum distortion is now -1.5%, if referred to an anamorphic model with 140 mm and 131.4 mm sagittal and tangential focal lengths respectively. If compared to a simplified pinhole model with 140 mm focal length, the maximum distortion is -6.5%.

4.2.1 WAC distortion measurements

WAC distortion has been measured in laboratory and verified in-flight using known star fields [13]. In laboratory [14] [15], the camera has been mounted on an ad hoc rotation stage in order to scan the FoV. The Azimuth (Az) and Elevation (El) angles of the WAC boresight with respect to the input collimated beam have been measured on a grid of 12×12 points covering the whole FoV of the camera. For each (Az, El) position, the corresponding image centroid coordinates on the detector have been determined and the position compared with the expected results.

In order to describe the system behavior, an optical model of the camera can be constructed where for each impinging direction $(\vartheta_x, \vartheta_y)$ the corresponding pixel position is associated. The coefficients of the ABCD matrix can be determined using both the measured data, and those predicted by a ray-tracing code simulation. Then, using a least square fit, the data can be interpolated with polynomial fitting as a function of the entrance angles or pixel positions; the model so realized is able to simulate the behavior of the camera to within a tenth of a pixel with a 3rd degree polynomial.

4.3 Distortion for STC on board the Bepicolombo ESA mission

The Stereo Imaging Channel STC of the SIMBIOSYS suite on board the Bepicolombo ESA-JAXA mission to Mercury is a single detector planetary stereocamera. STC is a double wide angle camera designed to image portions of the Mercury surface from two different perspectives, providing the panchromatic stereo image pairs required for generating the Digital Terrain Model of the planet surface [16].

The STC optical configuration (see Figure 9) is an original design, which can be thought to be composed by two independent elements: a fore-optics, consisting of two folding mirrors per each sub-channel, and a common telescope unit, which is an off-axis portion of a modified Schmidt design.

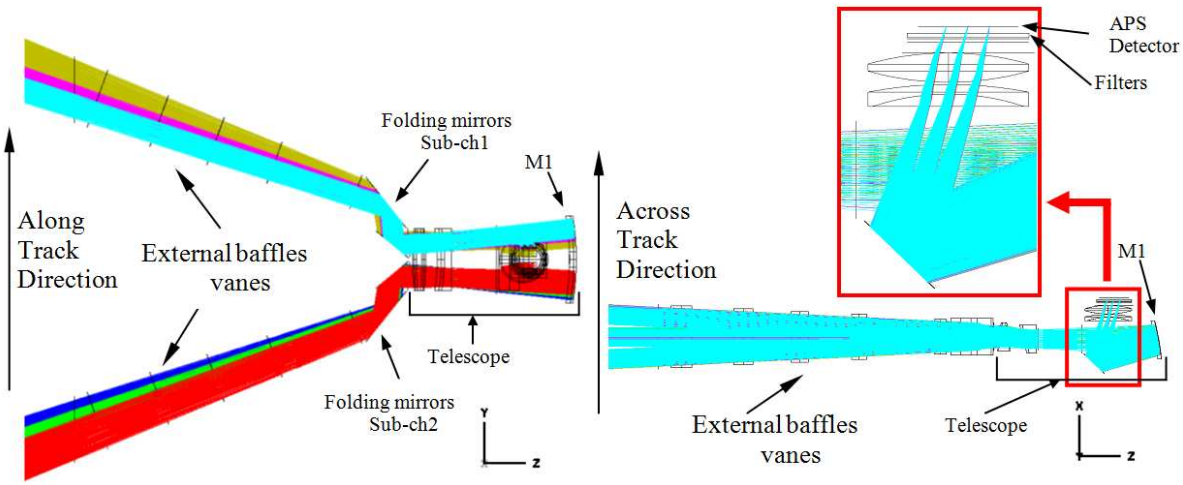

(a) (b)

Figure 9. Final overall STC optical layout. In (a) the configuration is viewed in the plane defined by the along track and nadir directions; in (b) the projection in the orthogonal plane, the one including across track and nadir directions, is given. In the inset, an enlarged view of the focal plane region helps to better follow the rays which are focalized on the APS detector.

The couple of folding mirrors redirects the ±20° (with respect to nadir) incoming beam chief rays to much smaller ±3.75° ones. The aperture stops of the two sub-channels are separated and are located off-axis with respect to the telescope primary mirror optical axis both in x and y directions, shifted respectively by 33.5 mm and ±13 mm. Therefore the design can essentially be described as an eccentric pupil one. A detail analysis of the Seidel aberrations for an off-centered pupil optical design and, in particular, of the distortion behavior is given in [17].

The design is such that the two sub-channels are symmetrical with respect to the xz plane (see Figure 9 for a definition of the xyz reference system). The two sub-channels share the same detector but they will observe the same region on the planet in different moments taking advantage of the spacecraft orbiting around the planet. Therefore, from the point of view of the acquisition, the two sub-channels can be considered as two independent cameras. The reference axis for each sub-channel is the boresight of the sub-channel itself.

In Figure 10, the distortion of the two sub-channels is shown on the detector plane. The dots represents the theoretical positions on the detector determined with a simplified pinhole model having 95 mm focal length centered on the boresight of the sub-channel and with a reference object plane orthogonal to the boresight axis. The crosses represent the corresponding calculated, via ray-tracing software, real image displacements, multiplied by a factor 20 to have the distortion effect visible. The effect of the off-axis displacement of the optical design along both x and y direction is evident in each sub-channel, as an asymmetrical smile effect. The maximum distortion on the two panchromatic filters is less than 0.2%.

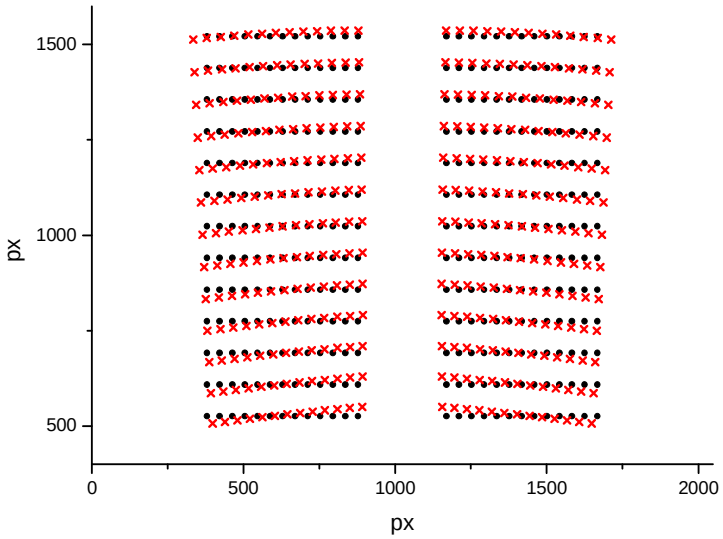

Figure 10. Distortion of the two STC sub-channels. Dots (•) represent the theoretical reference model images positions; crosses (×) represent the displacements, multiplied by a factor of 20, of the real images positions.

The distortion of the STC system has been measured on-ground during the instrument calibration activities using a lens collimator and a 45° degree folding mirror to scan each sub-channel FoV [18].

5. DISTORTION REMOVAL

Distortion effects can be corrected if the distorted image points can be relocated to their corresponding undistorted points. That is why accurate distortion models and practicable calibration methods are needed [19].

There are different distortion mapping methods [20] that can be chosen depending on the application; the distortion mapping process connects distorted image coordinates to the chosen undistorted ones and vice-versa. Then distortion removal is done warping the image from the real image coordinates to the nominal not distorted image coordinates.

To define the distortion mapping, firstly a set of distorted image coordinates (x_i, y_i) has to be known either from theoretical calculations or measurements done in laboratory or in-flight, as we have discussed in the previous paragraph. Secondly a not distorted reference model has to be considered (for example the pinhole model) to determine the corresponding set of perfect input coordinates (x_m, y_m).

A simple way to connect a known sample of (x_m, y_m) undistorted coordinates to their related (x_i, y_i) real coordinates is a polynomial fitting of the form:

$$x_m = \sum_{j,l} K_{x\,jl}\, x_i^{\,j} y_i^{\,l}$$
$$y_m = \sum_{j,l} K_{y\,jl}\, x_i^{\,j} y_i^{\,l} \tag{11}$$

Using a least squares estimation, the coefficients $K_{x\,jl}$ and $K_{y\,jl}$ of the polynomial functions can be determined.

Then an acquired image with pixel coordinates (x_{i_a}, y_{i_a}) can be unwarped to determine the undistorted corresponding image coordinates (x_{i_a}', y_{i_a}').

$$x'_{i_a} = \sum_{j=0}^{N} \sum_{l=0}^{N} K_{x\,jl}\, x_{i_a}^{\,j} y_{i_a}^{\,l}$$
$$y'_{i_a} = \sum_{j=0}^{N} \sum_{l=0}^{N} K_{y\,jl}\, x_{i_a}^{\,j} y_{i_a}^{\,l} \tag{12}$$

Finally, since the undistorted image has to be displayed, it has to be resampled on a regular grid. The interpolation can be done using nearest neighbour or bilinear convolution. The bilinear interpolation is a common method to improve the image quality during scaling or rotation processes. The algorithm of bilinear interpolation determines the intensity values of the undistorted pixel by taking a weighted sum of the intensity values of four nearest neighbour surrounding the calculated pixel position.

5.1 Distortion removal example

As an example of the distortion removal, an image of Mars obtained by the WAC before and after the distortion removal is depicted in Figure 11. This image has been taken during the Rosetta Mars fly-by in February 2007. It can be clearly seen that the original distorted image has anamorphic distortion as the planet is imaged as an ellipse, while after distortion removal it is circular.

A 135.7 mm focal length, which is the mean between the sagittal and tangential focal lengths on the boresight direction, has been chosen as reference. So the final undistorted images will look like as acquired by an ideal 135.7 mm focal length instrument with the projection plane orthogonal to the line of sight.

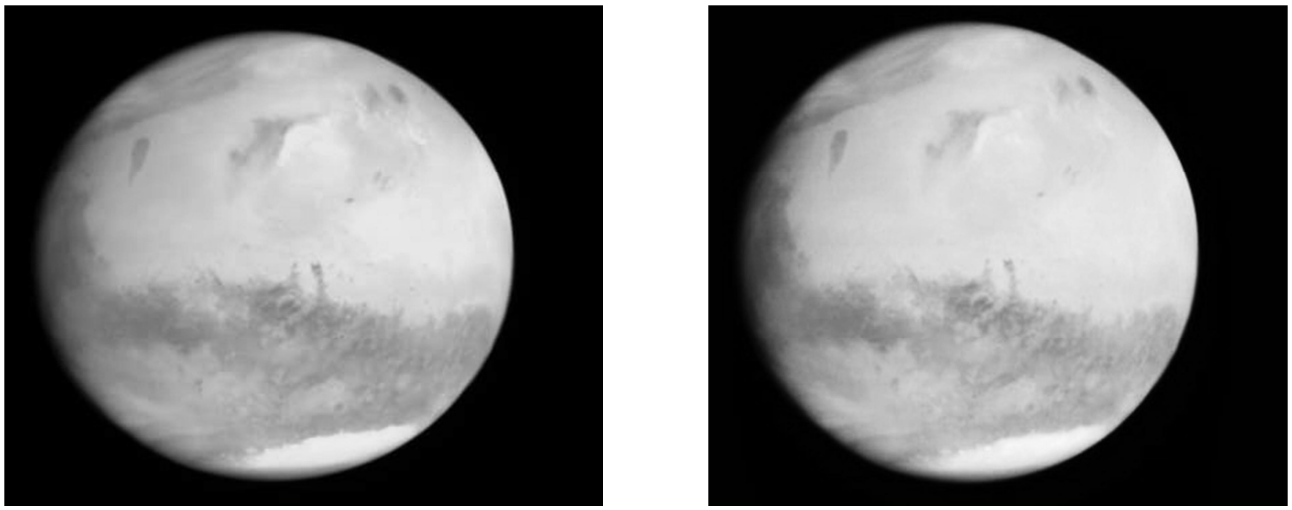

(a) (b)

Figure 11. Distortion removal example for the WAC. Image of the planet Mars before (a) and after (b) distortion removal. (Copyright ESA/Rosetta/MPS for OSIRIS Team MPS/UPD/LAM/IAA/SSO/INTA/UPM/DASP/IDA)

6. CONCLUSIONS

In this paper we have reviewed the classical definition of the distortion aberration given for simple axial symmetric systems; then the concept has been extended to off-axis non-symmetrical optical designs nowadays deeply used in a variety of optical applications, especially for astronomical imaging of extended objects like planets, asteroids and comets.

In a real optical system, the distortion has to be modelled, measured and removed. To model distortion means to be able to map incoming rays, i.e. points in the FoV, into their positions on the focal plane. This can be done theoretically starting from the ray-tracing of the optical configuration considered. The model can be verified and refined through measurements done in laboratory, during on-ground calibration, or in-flight, using stellar fields as references.

To undistort the image, the reference metrics of the ideal image has to be defined depending on the application, i.e. a reference model has to be used. For the purposes of our work, the discussion has been limited to the perspective and the equidistant models. The reference model enable to determine the ideal image position of the imaged points in the FoV. From the knowledge of a set of real imaged points positions (x_i, y_i), obtained theoretically or measured, and of their corresponding ideal positions (x_m, y_m), a warping of the image can be determined in order to map the acquired image points into an ideal non distorted image.

Two practical applications faced by the authors have been described and analyzed in detail. In both examples, the distortion has been compared to a reference simplified pinhole model. In the first case, for the off-axis FoV WAC of the OSIRIS instrument on board the Rosetta mission, the distortion is -6% and it is mainly anamorphic. In the second case, for the eccentric pupil STC of the SIMBIOSYS suite on board the BepiColombo mission, the distortion is 0.2% and it can be essentially described as an asymmetric smile effect.

Finally an example of image distortion removal for an image acquired in-flight with the WAC has been given.

ACKNOWLEDGMENTS

This activity has been partly realized under two Agenzia Spaziale Italiana (ASI) contracts to the Istituto Nazionale di Astrofisica (INAF) (WAC/Rosetta I/062/08/0 and BepiColombo I/022/10/0) and with the support of Selex ES (Campi di Bisenzio (FI) – Italy).

REFERENCES

[1] Rutten, H. and van Venrooij, M., [Telescope Optics], Willmann-Bell Inc., (1999).
[2] Schroeder, D. J., [Astronomical Optics – Second Edition], Academic Press, San Diego & London, (2000).
[3] Buchroeder, R. A., "Tilted-Component Telescopes. Part I: Theory", App. Opt. 9(9), 2169-2171, (1970).
[4] Hecht, E., [Optics – Fourth Edition], Addison Wesley, San Francisco, (2002).
[5] Kingslake, R. and Johnson, R. B., [Lens Design Fundamentals – Second Edition], Elsevier & SPIE Press, Amsterdam, (2010).
[6] Seidl, K., Knobbe, J., Schneider, D. and Lakner, H., "Distortion correction of all-reflective unobscured optical-power zoom objective", App. Opt. 49(14), 2712-2719, (2010).
[7] Pernechele, C. and Villa, F. A., "Hyper-hemispheric lens distortion model for 3D-imaging SPAD-array-based applications", to be published in Proc. SPIE 9626 (this issue) (2015).
[8] Fleck, M. M., "Perspective Projection: the Wrong Imaging Model", Technical Report 95-01, (1995).
[9] Yurevich, V. I., Grimm, V. A., Afonyushkin, A. A., Yudin, K. V. and Gorny, S. G., "Optical design and performance of F-Theta lenses for high-power and high-precision applications", to be published in Proc. SPIE 9626 (this issue) (2015).
[10] Keller, H.-U. et al., "OSIRIS - The scientific Camera System Onboard Rosetta", Space Sci. Rev. 128(1-4), 433-506 (2007).
[11] Flamini, E., Capaccioni, F., Colangeli, L., Cremonese, G., Doressoundiram, A., Josset, J.-L., Langevin, Y., Debei, S., Capria, M. T., De Sanctis, M. C., Marinangeli, L., Massironi, M., Mazzotta Epifani, E., Naletto, G., Palumbo, P., Eng, P., Roig, J. F., Caporali, A., Da Deppo, V., Erard, S., Federico, C., Forni, O., Sgavetti, M.,

Filacchione, G., Giacomini, L., Marra, G., Martellato, E., Zusi, M., Cosi, M., Bettanini, C., Calamai, L., Zaccariotto, M., Tommasi, L., Dami M., Ficai Veltroni, I., Poulet, F., Hello, Y. and The SIMBIO-SYS Team, "SIMBIO-SYS: The spectrometer and imagers integrated observatory system for the BepiColombo planetary orbiter", Planet. Space Sci. 58, 125-143 (2010).

[12] Naletto, G., Da Deppo, V., Pelizzo, M.-G., Ragazzoni, R. and Marchetti, E., "Optical design of the Wide Angle Camera for the Rosetta mission", App. Opt. 41(7), 1446-145 (2002).

[13] Tubiana, C., et al., "Scientific assessment of the quality of the OSIRIS images", Astronomy & Astrophysics, accepted for publication August 2015 (2015).

[14] Da Deppo, V., Naletto, G., Nicolosi, P., Zambolin, P., Pelizzo, M.-G. and Barbieri, C., "Optical performance of the Wide Angle Camera for the Rosetta mission: preliminary results", Proc. SPIE 4498, 248-257 (2001).

[15] Da Deppo, V. et al., "Preliminary calibration results of the Wide Angle Camera of the imaging instrument OSIRIS for the Rosetta mission", Proceeding of the 5th International Conference on Space Optics (ICSO 2004), 30 March - 02 April 2004, Toulouse, France, ESA SP-554, 191-198, (2004).

[16] Da Deppo, V., Naletto, G., Cremonese, G. and Calamai, L., "Optical design of the single-detector planetary stereo camera for the BepiColombo European Space Agency mission to Mercury", App. Opt. 49(15), 2910-2919 (2010).

[17] Korsch, D., [Reflective Optics], Academic Press, Boston, (1991).

[18] Da Deppo, V., Martellato, E., Simioni, E., Borrelli, D., Dami, M., Aroldi, G., Naletto G., Ficai Veltroni, I. and Cremonese, G., "Preliminary results of the optical calibration for the Stereo Camera STC onboard the BepiColombo mission", Proc. of ICSO 2014 – International Conference on Space Optics, Tenerife-Canary Islands-Spain, 7-10 October 2014, (2014).

[19] Devernay, F. and Faugeras, O., "Straight lines have to be straight", Mach. Vision Appl. 13, 14–24 (2001).

[20] Bauer, A., Vo, S., Parkins, K., Rodriguez, F., Cakmakci, O. and Rolland, J. P., "Computational optical distortion correction using a radial basis function-based mapping method", Opt. Exp. 20(14), 14906-14920 (2012).